ELSEVIER

Journal of Molecular Catalysis A: Chemical 153 (2000) 221–229

JOURNAL OF MOLECULAR CATALYSIS A: CHEMICAL

www.elsevier.com/locate/molcata

Photooxidation mechanism of dye alizarin red in TiO_2 dispersions under visible illumination: an experimental and theoretical examination

Guangming Liu [a], Xiangzhong Li [a], Jincai Zhao [a,*], Satoshi Horikoshi [b], Hisao Hidaka [b]

[a] *Institute of Photographic Chemistry, The Chinese Academy of Sciences, Beijing 100101, China*
[b] *Frontier Research Center for the Earth Environment Protection, Meisei University, 2-1-1 Hodokubo, Hino, Tokyo 191, Japan*

Received 21 May 1999; received in revised form 9 August 1999; accepted 13 September 1999

Abstract

Visible light-induced photocatalytic oxidation of the dye alizarin red (AR) has been examined in TiO_2 aqueous dispersions. The ESR spin-trapping technique was used to detect active oxygen radicals formed during in situ visible irradiation of AR/TiO_2 dispersions. Evidence for the production of superoxide ($O_2^{\cdot -}$ or $HOO^{\cdot}$) (formed in the reduction of O_2) and hydroxyl radicals ($^{\cdot}OH$) (formed by a multistep reduction) in the initial photoexcitation stage is presented. Meanwhile, the pathway of the photooxidation of AR is theoretically predicted on the basis of molecular orbital (MO) calculations by frontier electron densities and point charges on all the individual atoms of the dye. The relatively high negative point charges on the sulfonic oxygens lead to a strong adsorption of the dye onto the TiO_2 particle surface through the sulfonate function. The position of the dye molecule attacked by the active oxygen species (e.g., $O_2^{\cdot -}$ or $HOO^{\cdot}$ radicals) and/or O_2 is correlated with frontier electron densities, there is a perfect agreement between MO calculations and the results of experiments. A plausible mechanism of photooxidation under visible irradiation is discussed.

Keywords: Photooxidation; Dye; Visible light; TiO_2; Frontier electron density

1. Introduction

In recent years, textile dyes and other commercial colorants are becoming a focus of environmental remediation efforts [1,2]. Earlier studies [3–10] revealed that electron transfer processes occur between dyes and semiconductor particles under visible light irradiation. Utilizing of this process to degrade such colored organic pollutants as dyes has important applications because it can use visible light or sunlight. However, the photosensitized degradation of dyes in aqueous TiO_2 dispersion has been less frequently reported. Vinodgopal et al. [11] and Nasr et al. [12] reported the photooxidation of Acid Orange 7 and Naphthol Blue Black dyes preadsorbed on the surface of TiO_2 particles, and Ross et al. [13] examined the degradation of terbutylazine sensitized by rose bengal. Re-

* Corresponding author. Fax: +86-10-6487-9375.
E-mail address: jczhao@ipc.ac.cn (J. Zhao).

1381-1169/00/$ - see front matter
PII: S1381-1169(99)00351-9

cently, we reported the photodegradation of several dyes to CO_2 under exposure to visible light in aqueous TiO_2 dispersions [14–20]. The photodegradation mechanism under visible irradiation is proposed as follows (Eqs. 1–8):

$$\text{dye} + h\nu \rightarrow \text{dye}^* \quad (1)$$

$$\text{dye}^* + \text{TiO}_2 \rightarrow \text{dye}^{+\cdot} + \text{TiO}_2(\text{e}) \quad (2)$$

$$\text{TiO}_2(\text{e}) + \text{O}_2 \rightarrow \text{TiO}_2 + \text{O}_2^{\cdot -} \quad (3)$$

$$\text{H}^+ + \text{O}_2^{\cdot -} \leftrightarrow \text{HO}_2^{\cdot} \qquad pK_a = 4.69 \quad [21] \quad (4)$$

$$\text{HO}_2^{\cdot} + \text{HO}_2^{\cdot} \rightarrow \text{O}_2 + \text{H}_2\text{O}_2$$

$$K = 8.6 \times 10^5\ \text{M}^{-1}\,\text{s}^{-1} \quad [21] \quad (5)$$

$$\text{O}_2^{\cdot -} + \text{e} + 2\text{H}^+ \rightarrow \text{H}_2\text{O}_2 \quad (6)$$

$$\text{H}_2\text{O}_2 + \text{e} \rightarrow {}^{\cdot}\text{OH} + \text{OH}^- \quad (7)$$

$$\text{dye}^{+\cdot} + \text{O}_2\ (\text{or}\ \text{O}_2^{\cdot -}\ \text{or}\ {}^{\cdot}\text{OH})$$

$$\rightarrow \text{peroxide or hydroxyl intermediates}$$

$$\rightarrow \text{degraded or mineralized products} \quad (8)$$

The frontier electron theory of Fukui et al. [22,23] has already been applied to many fields in physical organic chemistry. In eletrophilic reactions, attention is focused on the two electrons of the highest occupied π molecular orbital (MO) of the ground state of the molecule, ''the frontier electrons'', which are distinct from other π electrons and play a decisive role in chemical reaction of those organic molecules. The position with the largest frontier electron density is most readily attacked by electrophilic or oxidizing species. So, we can obtain an illuminating explanation of the difference of reactivity at each position in a molecule. Predicting the reactivity of an organic molecule at a particular position by means of the LCAO MO method has been reported extensively [24–27]. Considerable progress has been made of late explaining the chemical reactivity of organic compounds by frontier electron density [28,29].

In a previous study [30], we examined the formation of intermediates in the photooxidation of the alizarin red (AR) dye in TiO_2 dispersions under visible light irradiation by means of Proton NMR, IR and gas chromatography/mass spectroscopy (GC–MS) techniques. However, the detailed photooxidation mechanism, especially the relationship between the photooxidation pathway and the molecular structure at the initial stage are still unknown. In the present paper, MO calculations have been carried out for each atom of the dye to assess frontier electron densities and point charges in order to seek some correlations between these simulation results and the experimental observation. Some essential relations were found between the reactivity and the density of the frontier electrons. In the case of photooxidation of AR, we show the applicability of the frontier electron theory to the theoretical interpretation of the visible light induced photooxidation mechanism.

2. Experimental

2.1. Materials

TiO_2 (P25, ca. 80% anatase, 20% rutile; BET area, ca. 50 $m^2\ g^{-1}$) were kindly supplied by Degussa. The spin trap reagent 5,5-dimethyl-1-pyrroline *N*-oxide (DMPO) was purchased from Sigma. The AR dye and other chemicals were all of analytical reagent grade quality and used without further purification. Deionized and doubly distilled water was used throughout this study. The pH of the solution was not adjusted and kept its original value (pH = 3.8).

2.2. Photoreactor and light source

A 500-W halogen lamp (Institute of Electric Light Source, Beijing) was used as the light source and positioned inside a cylindrical Pyrex vessel surrounded by a circulating water jacket (Pyrex) to cool the lamp. A cutoff filter was also placed outside the Pyrex jacket to remove

radiation below 410 nm completely and to ensure irradiation of the dispersion only by visible light wavelengths.

2.3. Procedures and analyses

AR aqueous solution (usually 50 ml) without or with a known amount of TiO_2 powder was put in a Pyrex vessel. Prior to irradiation the suspensions were magnetically stirred in the dark for ca. 30 min to ensure establishment of an adsorption/desorption equilibrium of dye on the TiO_2 surface. At given intervals of illumination, the TiO_2 powder was separated off by centrifuging and filtration through a Millipore filter (pore size 0.22 μm), the filtrates were analyzed by UV–Vis spectroscopy with a Shimadzu-160A spectrophotometer. Electron spin resonance (ESR) signals of spin-trapped paramagnetic species with DMPO were recorded with a Brucker ESP 300E spectrometer to examine the formation of active radical species, the irradiation source ($\lambda = 532$ nm) was an in situ Quanta-Ray ND:YAG pulsed (10 pulses/s) laser system. The settings for the ESR spectrometer were center field 3486.70 G, sweep width 100.0 G, microwave frequency 9.82 GHz, and power 5.05 mW. The GC–MS was obtained with a Trio-2000 spectrometer, equipped with a BPX70 column, size 28 m × 0.25 mm. The sample was prepared as follows: the TiO_2 particles were removed from a 50-ml of completely photoreacted solution (AR: 1×10^{-3} M; TiO_2: 100 mg) by centrifugation and filtration, subsequently, the solvent of the filtrate was removed (below 323 K) under reduced pressure. The remaining residue was dissolved in methanol for determination.

MO calculations were performed using the CAChe system from the MOPAC version 6 as implemented for a Power Macintosh computer. These MO calculations were carried out to the single determinant (Hartree–Fock) level, and optimal geometries of conformational minima were obtained at the AM1 level.

3. Results and discussion

3.1. Degradation of AR

AR aqueous solution in the absence of TiO_2 is considerably stable to visible irradiation in the wavelength range covering its main absorption band ($\lambda_{max} = 420$ nm). Curve (a) in Fig. 1 shows the concentration of the homogeneous AR solution (2×10^{-4} M) under visible light illumination for 2 h, exhibited almost no difference from the original value. Curve (c) gives the changes in the concentration of AR (2×10^{-4} M, 50 ml) in a TiO_2 (50 mg) dispersion at different time intervals during visible light irradiation. The absorption band of the dye diminished and finally disappeared, indicating that the degradation of AR and the destruction of the chromophoric structure of the AR dye. No new absorption bands appeared in the visible and ultraviolet regions. The temporal concentration changes of AR under visible illumination in the presence of TiO_2 illustrate that the degradation process follows zero order kinetics with a rate constant $k = 1.3 \times 10^{-6}$ M^{-1} min^{-1}, which further indicates that a saturated adsorption of AR dye molecules on the TiO_2 surface occurs (see below). It was also found that AR molecules both adsorbed on the TiO_2 surface and in the bulk solution disappeared completely within 2 h of irradiation. The strong adsorption favors the

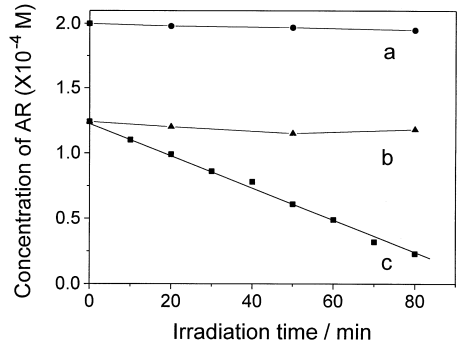

Fig. 1. Concentration of AR (2.0×10^{-4} M, 50 ml) changes with irradiation time in aqueous TiO_2 (50 mg) dispersions. (a) AR + light; (b) AR/TiO_2 in the dark; (c) AR/TiO_2 + light.

photodegradation of the dye on the TiO_2 surface, which can be seen in the result of Fig. 1 that AR (2×10^{-4} M, 50 ml) in the bulk solution completely degraded within 80 min of visible light illumination in the presence of 50 mg TiO_2 (adsorption of the dye on the surface was ca. 38%). In the previous study [19], the similar result was also confirmed that the rate of photodegradation of Rhodamine B was significantly accelerated by adding anionic surfactant sodium dodecylbenzenesulfonate (DBS) owing to enhancing the adsorption of the dye on the TiO_2 surface. Under our experimental conditions (pH = 3.8), the surface of the TiO_2 particles is positively charged ($pI_{TiO_2} = 6.8$ [31]), chemisorption of the dye AR on the TiO_2 surface takes place through the sulfonate group by coulombic forces, which is consistent with the results of MO calculation (see below) that the largest negative point charges are located at the sulfonic oxygens. Control experiments show that the AR dye did not degrade in the TiO_2 dispersions in the dark (curve b) or in a SiO_2 dispersion under visible irradiation under otherwise identical experimental conditions, which indicate that both visible light and TiO_2 semiconductor particles are indispensable to the degradation of the dye.

3.2. ESR measurements

The active oxygen radicals play an very important role in the initial photooxidation stage of the dye under visible irradiation in the presence of TiO_2. The potential for oxidation of the excited dye AR to the dye cationic radical ($E(D^*/D^{+\cdot}) = -1.57$ V vs. NHE) [32] lies above the conduction band edge of TiO_2 ($E_{cb} = -0.5$ V vs. NHE), the potentials for reduction of oxygen to superoxide ion ($E(O_2/O_2^{\cdot -}) = -0.15$ V vs. NHE) and for reduction of H_2O_2 to hydroxyl radical ($E(H_2O_2/{}^{\cdot}OH) = 0.3$ V vs. NHE) lie below the conduction band edge [33,34]. Therefore, the photogenerated electrons in the conduction band of TiO_2 injected from the excited dye are thermodynamically energetic to produce superoxide ion and hydroxyl radicals according to (Eqs. 2, 3 and 7). In order to examine and confirm the active oxygen radicals formed in the photooxidation of the dye under visible light irradiation as we proposed above, ESR spectra of DMPO spin-trapping adducts were in situ recorded following irradiation of AR/TiO_2 suspensions by pulsed laser light at $\lambda = 532$ nm. Fig. 2 shows the ESR spectra signals of spin-trapped DMPO-${}^{\cdot}OH$ radicals formed under visible irradiation of an aqueous AR/TiO_2 dispersion, the characteristic peak intensity of 1:2:2:1 evidenced that the ${}^{\cdot}OH$ radicals are indeed formed in the degradation of the dye under visible irradiation. The signals of DMPO-${}^{\cdot}OH$ radicals gradually increased with the irradiation time within the first 7 min and then remained unchanged with further irradiation for 20 min. However, unlike the mechanism of the photocatalytic degradation of organics under UV irradiation in which ${}^{\cdot}OH$ radicals predominantly result from the oxidation of H_2O and OH^- by positive holes in the valence band of TiO_2, the ${}^{\cdot}OH$ radicals under visible irradiation were produced via reduction of H_2O_2 (Eq. 7), which was formed by disproportionation (Eq. 5) and/or reduction of $O_2^{\cdot -}$ (Eq. 6) [21,34,35]. Because a relative large amount of H_2O_2 was observed in the system during visible illumina-

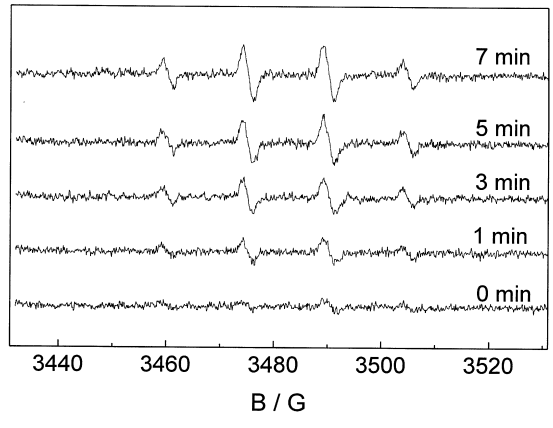

Fig. 2. ESR spectral changes of the DMPO-${}^{\cdot}OH$ adducts in the aqueous AR/TiO_2 dispersion (2×10^{-4} M, 0.4 ml, 4 mg TiO_2) under irradiation by a pulsed laser light (wavelength of excitation, 532 nm; 10 Hz); DMPO spin-trapping agent (1.24 mg).

tion as reported in our earlier work [30], the electrons on the conduction band of TiO_2 injected from the excited dye are mainly scavenged by adsorbed oxygen O_2 to produce $O_2^{\cdot -}$ and it is more difficult for the H_2O_2 to be reduced by the electrons in the conduction band of TiO_2 in competition with O_2. So the $^{\cdot}OH$ radicals formed by reduction of H_2O_2 although detectable, are only a small part of the active oxygen radicals produced under visible irradiation and not the main active species for the photooxidation of AR. This result is further substantiated in the following experiment that the photooxidation of the dye was not inhibited at all in the presence of isopropanol (1%), which is known as a good $^{\cdot}OH$ quencher [36]. We have not detected the species of $O_2^{\cdot -}$ or $HO_2^{\cdot}$ in aqueous AR/TiO_2 dispersion under visible illumination by DMPO spin-trap ESR measurements, because $O_2^{\cdot -}$ or $HO_2^{\cdot}$ could never accumulate to a concentration sufficiently large to be detected in water due to their rapid dismutation reaction [37]. In non-aqueous solvents, superoxide anion is relatively stable because disproportionation to give the peroxide diaion O_2^{2-} is highly unfavorable [21], so we carried out sequential ESR experiments in which the CH_3OH was used to substitute H_2O as the solvent to observe the generation of the superoxide radical. As illustrated in Fig. 3, characteristic signals of DMPO-$^{\cdot}$OOH or DMPO-$O_2^{\cdot -}$ adducts (six peaks with hyperfine splitting constants values of $\alpha^N = 13.3$ G, $\alpha_\beta^H = 10.4$ G [38]) are obtained in methanol solvent on irradiating a metholic AR/TiO_2 dispersion under the otherwise identical conditions as in Fig. 2. The signals intensity of DMPO-$^{\cdot}$OOH (or DMPO-$O_2^{\cdot -}$) adducts increased with the irradiation time in the 80-s irradiation and remained unchanged with further irradiation for 10 min. The above results infer that the superoxide radical does produce according to Eq. (3). In a control experiment, the degradation rate of AR was neither accelerated nor inhibited after addition of equivalent amount of H_2O_2. So, the dye cationic radical is oxidized in a multistep process mainly by active superoxide radicals and/or O_2 (Eq. 8).

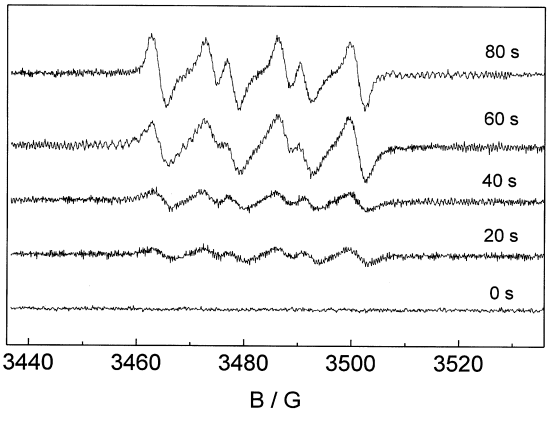

Fig. 3. ESR spectral changes of the DMPO-$^{\cdot}$OOH adducts in the AR/TiO_2 metholic dispersion with increasing the irradiation time under the otherwise identical conditions as in Fig. 2.

3.3. MO calculation

In order to predict further some details of the visible light induced photooxidative process through estimating the position of active oxygen radicals attack on the dye structure and the adsorption model of the dye on the TiO_2 surface, frontier electron densities and point charges of all individual atoms in the AR dye molecule were calculated using the CAChe system in the MOPAC program version 6 and are summarized in Table 1, the effect of solvent (H_2O) on the calculation results is also considered during the simulation process. As expected, the most negative point charges are located on the oxygen atoms O20, O21 and O22 of the sulfonate group, the TiO_2 particle surface is positively charged at pH ca. 3.8 under the experimental conditions (the isoelectric point of TiO_2 P25 is p$I = 6.8$ [31]). Therefore, the chemisorption of the dye on the surface of TiO_2 is through the sulfonic oxygen, the strong adsorption of the dye (see above) can be explained from the greater values of the negative point charges (-1.087) on the sulfonic oxygen atoms. Similar results were also reported that the molecules with a sulfonate group such as anionic surfactant DBS can be

adsorbed strongly on the TiO_2 surface through the sulfonate group [31,39]. The characteristics of frontier electron densities in the AR molecule are different from that of the point charges, as implied in Table 1, the highest frontier electron density in AR molecule is at the C9 (0.172) but the point charge on this carbon is only −0.165; as well, the O21 with the largest negative point charge has only a smaller frontier electron density (0.059). As we noted above, under visible illumination, the excited dye molecule injects an electron to the conduction band of TiO_2 to form dye cationic radical, the photooxidation path of the dye depends closely on the atom donating the electron in the molecule, which is subsequently attacked by active oxygen radicals or O_2 to result in the photooxidation of the dye. We postulate that the atom with the largest frontier electron density in ground state of the dye molecule most easily donates the electron to the conduction band of TiO_2 when the dye is excited by visible light.

Table 1
Frontier electron densities and charge calculations of AR using the CAChem method from the MOPAC system
The calculation values of H atoms of AR were omitted in this table.

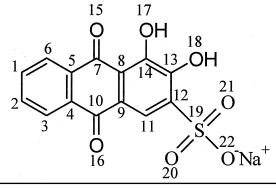

Atom	Frontier electron density	Point charges
C1	0.105	−0.132
C2	0.103	−0.132
C3	0.041	−0.097
C4	0.137	−0.098
C5	0.137	−0.099
C6	0.040	−0.099
C7	0.071	0.308
C8	0.061	−0.118
C9	0.172	−0.165
C10	0.071	0.312
C11	0.093	0.013
C12	0.096	−0.742
C13	0.151	0.139
C14	0.161	0.074
O15	0.079	−0.285
O16	0.094	−0.307
O17	0.076	−0.232
O18	0.095	−0.311
S19	0.000	2.886
O20	0.077	−1.046
O21	0.059	−1.087
O22	0.078	−1.046

The photooxidation of the dye is initiated by losing an electron in excited state and followed by an attack of the active oxygen radicals, and the primary positions of the dye molecule lost electrons and attacked by these active oxygen species will be those atoms with the largest frontier electron density, so the distribution of the frontier electron density in the dye molecule will determine the photooxidation path of the dye in the initial photooxidation stage. For AR the largest frontier electron density is distributed at C9 atom in the molecule structure, so the C9 atom of the dye molecule easily donates an electron to the conduction band of TiO_2 when the dye is excited and then forms cationic radical ($RC^{+\cdot}$), which subsequently is attacked at the C9 position by the active oxygen radicals and/or O_2, leading to the formation of organoperoxides $(RCOO^{\cdot})^{+}$ and destruction of the chromophoric function. These organoperoxides (or hydroxyl intermediates) further degrade to the final products via complicated steps. According to the above results of MO calculation, the dye AR is probably oxidized and cleaved to form benzoic acid-type intermediates and other small species after attack of the active oxygen species on the C9. So that the density distribution of the frontier electrons will determine the configuration of the transition complex for the reaction and furthermore the photooxidation pathway of the dye under visible illumination. In the following, the photooxidation mechanism of AR will be further discussed by comparing the theoretic MO calculation data with experimental results.

3.4. Photooxidation mechanism

The major degraded component in the photooxidation of AR confirmed by the GC–MS

analysis is the fragment phthalic acid [30] besides of CO_2, well consistent with the results predicted by MO calculation. The mass spectrum of the main final product gave m/e 148 $[M - H_2O]^+$, 104 $[M - COOHOH]^+$, 76 $[M - (COOH)_2]^+$, where m/e 166 $[M]^+$ of phthalic acid was not observed due to the weak signal intensity of $[M]^+$. The mineralization extent of the dye in the same system was ca. 30%, confirmed by COD_{Cr} measurement and the extent of conversion to SO_4^{2-} was ca. 35%, assayed by ion chromatography [30]. These data indicate that the dye is at least partly mineralized. From the results above, we can see that there is a perfect agreement between calculation and the results of experiments in the case of the AR photooxidation, the dye in the form of cationic radical is attacked at the C9 position by active oxygen radicals and/or O_2 in the initial photooxidation process under visible irradiation and this leads to the formation of phthalic acid as we predicted above. The density distribution of the frontier electrons at each atom in the molecule can account for the discriminating reactivity of each position of the dye in the initial oxidation stage. The position with the largest density of the frontier electrons indicates the most reactivity position and the position most easily donating electrons in the excited state and meanwhile the most readily attacked position by active oxygen radicals and/or O_2. As illustrated in Scheme 1, the AR molecule adsorbed on the surface of TiO_2 is excited and then injects an electron to the conduction band of TiO_2 to form

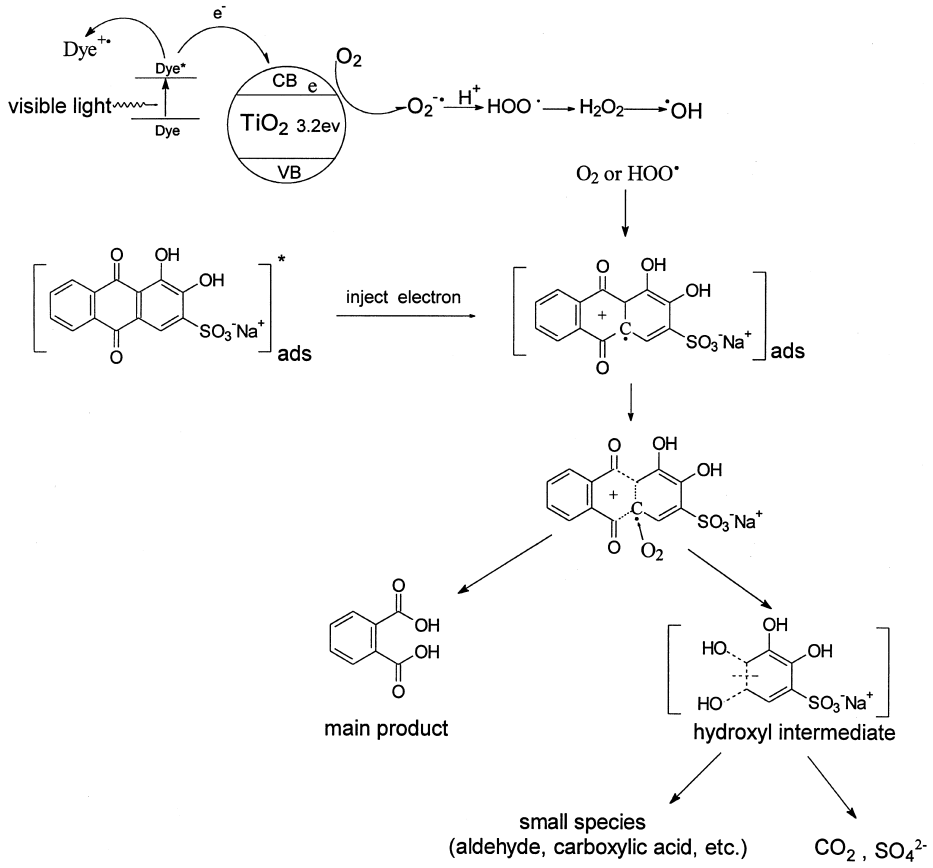

Scheme 1. Proposed photooxidation pathway for AR under visible light irradiation in TiO_2 aqueous dispersions.

dye cationic radical. The electron in the TiO_2 conduction band is scavenged by the O_2 preadsorbed on the TiO_2 surface to form superoxide ion radical $O_2^{\cdot -}$, which further converts to $HOO^{\cdot}$, H_2O_2 and $^{\cdot}OH$ species via a series of protonation, disproportionation and reduction steps. O_2 play an very important role in the preventing recombination of $dye^{+\cdot}$ and electrons and in the formation of active oxygen radicals, as evidenced by above experiments. The injected electron comes from the C9 atom with the largest frontier electron density in the AR molecule (as postulated in Section 3.3). The C9 atom of cationic radical is attacked/or combine with the active oxygen radicals and/or O_2 to result in the formation of organoperoxide intermediate, which is very unstable. The decomposition of this organoperoxide intermediate leads to the destruction of the conjugated system of the dye. The dye molecule is cleaved into two parts by attacking of O_2 and/or active oxygen radicals, one part is oxidized to phthalic acid, which no longer degrades since it can not absorb visible light and is relatively stable under the experimental conditions; another part is oxidized to hydroxyl intermediates and finally mineralized to CO_2, SO_4^{2-} and small organic species via a series of complicated oxidation reactions of transient intermediates (aldehyde and/or carboxylic acid as evidenced by HNMR and IR measurements [30]).

4. Conclusions

The photooxidation of AR has been examined experimentally, comparing with theoretical MO simulation of frontier electron densities and point charges on all the individual atoms of the dye molecule. The ESR spin-trapping technique confirmed that active oxygen radicals of superoxide ($O_2^{\cdot -}$ or $HOO^{\cdot}$) and hydroxyl radicals ($^{\cdot}OH$) are generated during visible irradiation of AR/TiO_2 dispersions in the initial photooxidation stage. The negative point charges on the sulfonic oxygens inferred that adsorption of AR to the TiO_2 surface takes place through the sulfonate function. The position C9 of AR molecule with the largest frontier electron density is most readily attacked by the active oxygen radicals and/or O_2, which is well consistent with the experimental results that phthalic acid was formed as a main photooxidation products. The frontier electron density calculations may be very useful in predicting the attack position of the dye by active oxygen radicals and rationalizing the predominant primary events in photocatalysis under visible light irradiation.

Acknowledgements

The generous financial support of this work from the National Natural Science Foundation of China (Nos. 29677019, 29725715, and 29637010), the Foundation of the Chinese Academy of Sciences and the China National Committee for Science and Technology (to J.Z.) is gratefully acknowledged. The work in Tokyo is sponsored by a Grant-in-Aid for Scientific Research from the Japanese Ministry of Education (No. 10640569; to H.H.). We are also grateful to Prof. J. Chen for her measurements of the ESR spectra.

References

[1] R. Ganesh, G.D. Boardman, D. Michelson, Water Res. 28 (1994) 1367.
[2] E.J. Weber, R.L. Adams, Environ. Sci. Technol. 29 (1995) 113.
[3] R. Rossetti, L.E. Brus, J. Am. Chem. Soc. 106 (1984) 4336.
[4] K. Vinodgopal, P.V. Kamat, J. Photochem. Photobiol. A: Chem. 83 (1994) 141.
[5] P.V. Kamat, S. Das, K.G. Thomas, M.V. George, Chem. Phys. Lett. 178 (1991) 75.
[6] J. He, J. Zhao, T. Shen, H. Hidaka, N. Serpone, J. Phys. Chem. 101 (1997) 9027.
[7] J. He, J. Zhao, H. Hidaka, N. Serpone, J. Chem. Soc., Faraday Trans. 94 (1998) 2375.
[8] P. Qu, J. Zhao, T. Shen, H. Hidaka, Colloids Surf., A 138 (1998) 39.

[9] P.V. Kamat, K. Vinodgopal, in: D.F. Ollis, H. Al-Ekabi (Eds.), Photocatalytic Purification and Treatment of Water and Air, Elsevier, Amsterdam, The Netherlands, 1993, p. 8.
[10] A.L. Linsebigler, G. Lu, J.J.T. Yates, Chem. Rev. 95 (1995) 735.
[11] K. Vinodgopal, D. Wynkoop, P.V. Kamat, Environ. Sci. Technol. 30 (1996) 1660.
[12] C. Nasr, K. Vinodgopal, L. Fisher, S. Hotchandani, A.K. Chattopadhya, P.V. Kamat, J. Phys. Chem. 100 (1996) 8436.
[13] H. Ross, J. Bendig, S. Hecht, Sol. Energy Mater. Sol. Cells 33 (1994) 475.
[14] F. Zhang, J. Zhao, L. Zang, T. Shen, H. Hidaka, E. Pelizzetti, N. Serpone, J. Mol. Catal. A: Chem. 120 (1997) 173.
[15] F. Zhang, J. Zhao, T. Shen, H. Hidaka, E. Pelizzetti, N. Serpone, Appl. Catal. B: Environ. 15 (1998) 147.
[16] J. Zhao, K. Wu, T. Wu, H. Hidaka, N. Serpone, J. Chem. Soc., Faraday Trans. 94 (1998) 673.
[17] P. Qu, J. Zhao, T. Shen, H. Hidaka, J. Mol. Catal. A: Chem. 129 (1998) 257.
[18] T. Wu, G. Liu, J. Zhao, H. Hidaka, N. Serpone, J. Phys. Chem. B 102 (1998) 5845.
[19] J. Zhao, T. Wu, K. Wu, K. Oikawa, H. Hidaka, N. Serpone, Environ. Sci. Technol. 32 (1998) 2394.
[20] T. Wu, T. Lin, J. Zhao, H. Hidaka, N. Serpone, Environ. Sci. Technol. 33 (1999) 1379.
[21] D.T. Sawyer, J.S. Valentine, Acc. Chem. Res. 14 (1981) 393.
[22] K. Fukui, T. Yonezawa, H. Shingu, J. Chem. Phys. 20 (1952) 722.
[23] K. Fukui, T. Yonezawa, C. Nagata, J. Chem. Phys. 21 (1953) 174.
[24] G.W. Wheland, J. Am. Chem. Soc. 64 (1942) 900.
[25] H.C. Longuet-Higgins, J. Chem. Phys. 18 (1950) 283.
[26] G.W. Wheland, L. Pauling, J. Am. Chem. Soc. 57 (1935) 2086.
[27] H.C. Longuet-Higgins, C.A. Coulson, Trans. Faraday Soc. 43 (1947) 87.
[28] H. Hada, C. Honda, Photogr. Sci. Eng. 19 (1975) 363.
[29] S. Horikoshi, N. Serpone, J. Zhao, H. Hidaka, J. Photochem. Photobiol. A: Chem. 118 (1998) 123.
[30] G. Liu, T. Wu, J. Zhao, H. Hidaka, N. Serpone, Environ. Sci. Technol. 33 (1999) 2081.
[31] J. Zhao, H. Hidaka, A. Takamura, E. Pelizzetti, N. Serpone, Langmuir 9 (1993) 1646.
[32] L. Meites, P. Zuman, in: CRC Handbook Series in Organic Electrochemistry I CRC Press, 1976, p. 590.
[33] C.D. Jaeger, A.J. Bard, J. Phys. Chem. B 83 (1979) 3146.
[34] H. Noda, K. Oikawa, H. Kamada, Bull. Chem. Soc. Jpn. 65 (1992) 2505.
[35] D.H. Chin, G. Chiericato, E.J. Nanni, D.T. Sawyer, J. Am. Chem. Soc. 104 (1982) 1296.
[36] C. Richard, J. Photochem. Photobiol. A: Chem. 72 (1993) 179.
[37] J.M. Mccordm, I. Fridovich, J. Biol. Chem. 244 (1969) 6049.
[38] J.R. Harbour, M.L. Hair, J. Phys. Chem. 82 (1978) 1397.
[39] T. Imae, K. Muto, S. Ikeda, Colloid Polym. Sci. 269 (1991) 43.